

High performance amorphous Zn-Sn-O: impact of composition, microstructure, and thermal treatments in the optoelectronic properties

Monica Morales-Masis^{*a}, Esteban Rucavado^a, Quentin Jeangros^{a,b}, Federica Landucci^a, Aïcha Hessler-Wyser^a, Christophe Ballif^a

^a Ecole Polytechnique Fédérale de Lausanne (EPFL), Institute of Microengineering (IMT), Photovoltaics and Thin-Film Electronics Laboratory, Rue de la Maladière 71b, 2002 Neuchâtel, Switzerland

^b University of Basel, Department of Physics, Klingelbergstrasse 82, Basel CH-4056, Switzerland

ABSTRACT

Zinc and tin oxides are both earth-abundant materials with demonstrated applicability as electrodes in several optoelectronic devices. The presence of grain boundaries in these polycrystalline films generally limits the electron mobility. By a combinatorial study of ZnO and SnO₂, a transparent conducting amorphous zinc tin oxide (ZTO) electrode, free of grain boundaries, with a dense (void-free) microstructure has been developed. We show how tuning the stoichiometry (Zn_{4.5}Sn_{30.2}O_{65.3}) and film's microstructure during sputtering deposition, allows achieving electron mobilities up to 25 cm²/Vs and free carrier concentrations of $\sim 7 \times 10^{19}$ cm⁻³. The effects of post-deposition thermal treatments are furthermore studied. The ZTO films keep their dense amorphous microstructure upon annealing up to 500 °C, as confirmed by cross-section TEM and XRD, while presenting a clear improvement in electron mobility up to 35 cm²/Vs when annealed in oxygen-rich atmospheres.

Keywords: Zinc tin oxide, amorphous TCOs, carrier transport, microstructure

1. INTRODUCTION

Zinc oxide (ZnO) and tin oxide (SnO₂) are both known transparent conductive oxides (TCOs), largely studied since the 1950's.¹ ZnO, on one side, has been widely used as electrode in photovoltaics, due to its excellent optoelectronic properties as well as the tunability of its microstructure.^{2,3} However, ZnO is not chemically stable, restricting its application in devices for which the substrate is the TCO layer and chemical cleaning is required, e.g. organic light emitting diodes (OLEDs). SnO₂ on the other hand, is a chemically stable TCO,⁴ however, it presents high free carrier absorption (FCA) when dopants are introduced (e.g. F-doping).^{5,6} Zn-Sn-O (ZTO) multi-compounds have also been reported in literature for application as active channel in flexible thin film transistors, due to its amorphous structure and low free carrier concentration.^{7,8} Due to its limited conductivity, ZTO has not been widely exploited as a transparent electrode. In this manuscript, the development of ZTO with the specific composition of Zn_{4.5}Sn_{30.2}O_{65.3} that has an optimized transparency and conductivity is presented. The effects of the microstructure and post-deposition thermal treatments on the optoelectronic properties are furthermore discussed. The development of these amorphous ZTO films with sufficient conductivity and low surface roughness has enabled their application in flexible OLEDs when applied in combination with metal grids⁹. On the other hand, the high thermal stability up to 500 °C together with an improved conductivity has enabled the application of a-ZTO as recombination layer in silicon/perovskite tandems solar cells.¹⁰

2. EXPERIMENTAL DETAILS

2.1. Combinatorial sputtering from ZnO and SnO₂ targets.

For the co-sputtering deposition of the films, a ZnO and a SnO₂ 4-inch diameter targets were used. The targets were facing each other and simultaneously ignited using RF magnetron sputtering in an Oerlikon Clusterline System. The RF power density was 5.1 W/cm² for the SnO₂ target and 1.9 W/cm² for the ZnO:Al target. The co-sputtering deposition was

performed at a process pressure of 5.5×10^{-3} mbar with an oxygen to total flow ratio, $r(\text{O}_2) = \text{O}_2/(\text{Ar} + \text{O}_2)$, of 0.34%. All samples were deposited at a substrate temperature of 60°C onto glass substrates ($4 \times 8 \text{ cm}^2$).

2.2. Sputtering from a single target of Zn-Sn-O with optimized composition.

Once the highest conductivity phase and composition of the Zn-Sn-O co-sputtered films were identified, the fabrication of a customized target was performed. The sputtering deposition was performed at a power density of 2.6 W/cm^2 at a $r(\text{O}_2)$ of 0.84% as optimized in ref.⁹. Two working pressures were investigated, i.e. 1×10^{-3} and 5×10^{-4} mbar.

2.3. Characterization

The structural properties of the layers were characterized by transmission electron microscopy (TEM). For the TEM examination, the cross-sections were prepared using the conventional focused ion beam (FIB) lift-out technique (Zeiss Nvision). The crystallographic properties of the films were determined using selected-area electron diffraction (SAED), while the structural assessment of the films involved the acquisition of scanning TEM (STEM) bright-field (BF) and high-angle annular dark-field (HAADF) images. The chemical composition of the films was determined by Rutherford backscattering (RBS) and STEM energy-dispersive X-ray spectroscopy (EDX). Resistivity (ρ), Hall mobility (μ_{Hall}) and free-carrier concentration (N_e) were determined by Hall-effect measurements using the van der Pauw configuration. Optical transmittance and reflection spectra in the range of 320 to 2000 nm were measured using a UV-Vis-NIR spectrophotometer equipped with an integrating sphere.

3. RESULTS AND DISCUSSION

The development of the indium-free films started by a combinatorial screening of Zn-Sn-O compounds by co-sputtering deposition. Figure 1.a presents a schematic diagram of the targets and glass substrate positioning for the combinatorial growth. The five areas marked in colors were analyzed by EDX, and the measured Sn/Zn ratios were 22.9, 10.7, 4.2, 1.4 and 0.7 from left to right. The sheet resistance measured were 1000, 350, 240, 360, 1000 Ohm sq^{-1} also from left to right. The thickness of the films decreased progressively from 300 nm on the left to 250 nm on the right. A full analysis of the microstructure of each of these films is presented in ref.⁹. Figure 1b and 1c show the rest of the process flow, including the fabrication of a single target with the composition of the films that presented higher conductivity, i.e. of Zn = 6.3 at.%, Sn = 27.8 at.%, and O = 65.9 at.% (Sn/Zn ratio of 4.4) as determined by RBS, and the optimization of the sputtering parameters, mainly working pressure and oxygen flow ratio.

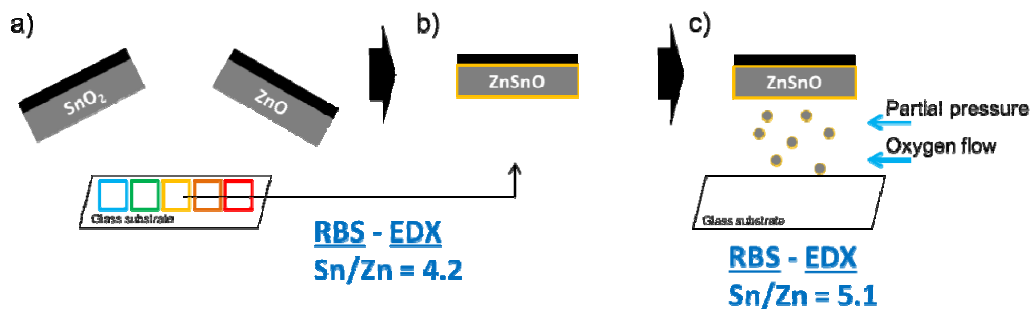


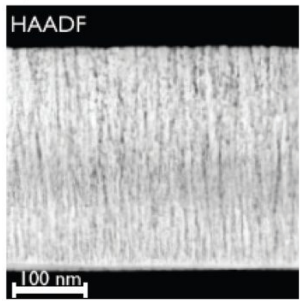
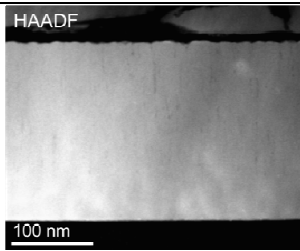
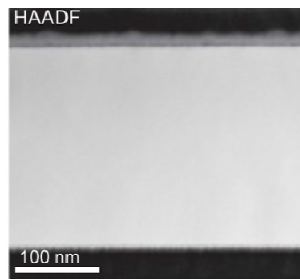
Figure 1. Process flow for the development of amorphous ZTO films with improved conductivity. a) Combinatorial study of material phases formed from SnO_2 and ZnO targets, b) selection of the highest conductive phase (lower sheet resistance), and c) optimization of sputtering parameters using a single target with the determined composition.

3.1 Microstructure vs optoelectronic properties: from co-sputtering deposition to single-target sputtering

Table 1 summarizes the electrical properties and the corresponding microstructure of the co-sputtered and single-target sputtered films. All the films are amorphous. However, from the cross-section view, the co-sputtered films present a high density of nanovoids, while the films deposited from the fabricated ZTO single target are denser. In fact, deposition at a low working pressure (5×10^{-4} mbar) results in the formation of dense, void-free ZTO films. When comparing with the

electrical properties and considering the small change in carrier concentration, we propose that the improvement in electron mobility is linked to the improvement of the films quality, i.e. the clear reduction of voids in the films. It is important to mention here that the co-sputtered films, as well as the single target-sputtered films present a uniform element (Sn, Zn, O) distribution across the thickness of the layer.^{9,11} The dense amorphous microstructure also enables higher strength to mechanical bending in comparison to polycrystalline materials as demonstrated in ref.¹².

Table 1. Evolution of the electrical properties of ZTO films from co-sputtered films to low-pressure sputtering deposition.

TCO	Microstructure	Phase	Sn/Zn	N_e (10^{19} cm^{-3})	μ (cm^2/Vs)	σ ($\Omega^{-1}\text{cm}^{-1}$)
ZTO Co- sputtered		Amorphous High density of voids	4.4	5	12	110
ZTO Single target sputtering Working pressure: 1E-3 mbar		Amorphous Low density of voids	5	7.7	18	220
ZTO Single target sputtering Working pressure: 5E-4 mbar		Amorphous Dense structure, no presence of voids detected	5	7.3	21	245

3.2 Post-deposition thermal treatments

Following the optimization of the a-ZTO by their microstructure and composition, the effects of post-deposition treatments were studied. Previously it was demonstrated that a hydrogen plasma treatment improves the conductivity of co-sputtered ZTO films, but slightly sacrificing the optical properties¹¹. Using the optimized ZTO layers (sputtered from a single target), annealing studies were performed in oxygen-rich and hydrogen-rich atmospheres. The conductivity, carrier density and Hall mobility before and after annealing in air or in hydrogen atmospheres are presented in Table 2.

Table 2. Electrical properties of the a-ZTO films as-deposited and after post-thermal treatments in oxygen and hydrogen-rich atmospheres.

a-ZTO treatment	Phase	N _e (10 ¹⁹ cm ⁻³)		μ (cm ² /Vs)		σ (Ω ⁻¹ cm ⁻¹)	
		Air	H ₂	Air	H ₂	Air	H ₂
ZTO As-deposited	Dense amorphous structure ⁹	7		21		245	
Post-annealing							
ZTO Annealed at 150 °C 30 min	Amorphous ^{13,14}	10	8.5	23	24	368	327
ZTO Annealed at 500 °C 30 min	Amorphous ^{13,14}	6	16	35	24	336	614

3.3. Optical properties

The absorbance of the films, calculated from transmittance (TT) and reflectance (TR) measurements ($A = 100 - TT - TR$) are presented in Fig. 2. As observed in the figure, the evolution of the optical properties to lower absorbance values in the visible range goes in-line with the improvement of the film quality, and with it, the improvement of the electrical properties as shown in Table 2. The only exception is the film annealed at 500 °C in a H₂ atmosphere, which presents the highest conductivity with a trade-off on the optical properties. The highest conductivity of the H₂-annealed sample is due to the strong increase in carrier concentration, possibly due to hydrogen doping in the films. Increasing the doping causes the increase in absorbance, both in the visible and in the NIR (free carrier absorption). In the case of air-annealed samples at high temperatures, opposite to the H₂ annealing, we see a strong increase in mobility, but lower carrier concentration. This can be interpreted by oxidation of the films, reducing the density of oxygen vacancies and with it also a clear reduction of the defect density in the films.¹⁴ These defects can be due to disorder, loose metal bonds, and/or metal-metal pairs or nanoclustering that create levels below the band gap generating absorption levels. This has been described theoretically by Korner et al in ref.¹⁵. In fact, by annealing the films at high temperatures (i.e. 500 °C) in oxygen-rich atmosphere (air in the present case), we see that the subgap absorbance at 500 nm is clearly reduced. A complete study of the link between subgap states and optoelectronic properties is found in ref.¹⁴.

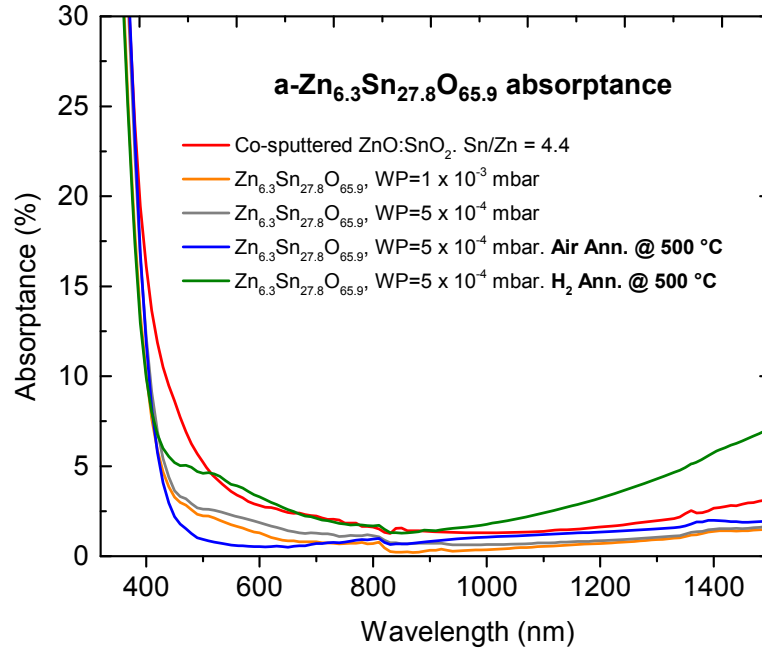


Figure 2. Absorbance spectra of a-ZTO layers: from co-sputtered, to the optimized sputtered layers from a single target, and post-annealed at 500 °C in air and H₂ atmospheres. (WP= working pressure)

4. CONCLUSION

We have developed a sputtered amorphous Zn-Sn-O TCO deposited at low temperature with electron mobilities of up to 21 cm²/Vs and a conductivity of 245 Ω⁻¹cm⁻¹. These films were obtained by optimizing the microstructure of Zn-Sn-O, i.e. by forming dense, void-free layers. Post-deposition thermal treatments enable a further improvement of the conductivity of the films. Hydrogen annealing at high temperatures results in a strong increase in carrier density up to 1.6E20 cm⁻³ due to hydrogen doping. The hydrogen doping allowed reaching the highest conductivity of 614 Ω⁻¹cm⁻¹, but with a trade-off on the optical properties. On the other hand, annealing in oxygen-rich atmospheres at 500 °C enables a pronounced increase in mobility of up to 35 cm²/Vs, whilst keeping a carrier density of 6E19 cm⁻³. Considering that the film is amorphous even after annealing at 500 °C, the obtained mobility of 35 cm²/Vs is remarkable. It is proposed that the increased mobility together with the excellent optical properties from the visible to the near infrared both result from the improvement in the film quality as well as the reduction of oxygen vacancies originally source of sub-band gap absorption centers.

Acknowledgements

This work is funded through the Swiss National Science Foundation (SNSF) Sinergi project DisCO.

*monica.moralesmasis@epfl.ch;

REFERENCES

- [1] Ellmer, K., "Past achievements and future challenges in the development of optically transparent electrodes," *Nat Photon* 6, 809 (2012).
- [2] Fanni, L., Aebersold, B. A., Alexander, D. T. L., Ding, L., Masis, M. M., Nicolay, S. and Ballif, C., "c-texture versus a-texture low pressure metalorganic chemical vapor deposition ZnO films: Lower resistivity despite smaller grain size," *Thin Solid Films* 565, 1 (2014).
- [3] Fanni, L., Aebersold, A. B., Morales-Masis, M., Alexander, D. T. L., Hessler-Wyser, A., Nicolay, S., Hebert, C. and Ballif, C., "Increasing Polycrystalline Zinc Oxide Grain Size by Control of Film Preferential Orientation," *Crystal Growth & Design* 15, 5886 (2015).
- [4] Gordon, R. G., "Criteria for choosing transparent conductors" *Mrs Bulletin* 25, 52 (2000).
- [5] Peelaers, H., Kioupakis, E. and Van de Walle, C. G., "Fundamental limits on optical transparency of transparent conducting oxides: Free-carrier absorption in SnO₂," *Appl. Phys. Lett.* 100 (2012).
- [6] Yates, H. M., Gaskell, J. M., Thomson, M. E., Sheel, D. W., Delaup, B. and Morales-Masis, M., "APCVD of dual layer transparent conductive oxides for photovoltaic applications," *Thin Solid Films* 590, 260 (2015).
- [7] Zhu, Q., Ma, Q., Buchholz, D. B., Chang, R. P. H., Bedzyk, M. J. and Mason, T. O., "Structural and physical properties of transparent conducting, amorphous Zn-doped SnO₂ films," *J. Appl. Phys.* 115, 033512 (2016).
- [8] Yu, X. G., Marks, T. J. and Facchetti, A., "Metal oxides for optoelectronic applications" *Nature Materials* 15, 383 (2016).
- [9] Morales-Masis, M., Dauzou, F., Jeangros, Q., Dabirian, A., Lifka, H., Gierth, R., Ruske, M., Moet, D., Hessler-Wyser, A. and Ballif, C., "An Indium-Free Anode for Large-Area Flexible OLEDs: Defect-Free Transparent Conductive Zinc Tin Oxide," *Advanced Functional Materials* 26, 384 (2016).
- [10] Werner, J., Walter, A., Rucavado, E., Moon, S.-J., Sacchetto, D., Rienaecker, M., Peibst, R., Brendel, R., Niquille, X., De Wolf, S., Löper, P., Morales-Masis, M., Nicolay, S., Niesen, B. and Ballif, C., "Zinc tin oxide as high-temperature stable recombination layer for mesoscopic perovskite/silicon monolithic tandem solar cells," *Appl. Phys. Lett.* 109, 233902 (2016).
- [11] Morales-Masis, M., Ding, L., Dauzou, F., Jeangros, Q., Hessler-Wyser, A., Nicolay, S. and Ballif, C., "Hydrogen plasma treatment for improved conductivity in amorphous aluminum doped zinc tin oxide thin films," *APL Materials* 2, 096113 (2014).
- [12] Dauzou, F., Bouten, P. C. P., Dabirian, A., Leterrier, Y., Ballif, C. and Morales-Masis, M., "Mechanical integrity of hybrid indium-free electrodes for flexible devices," *Organic Electronics* 35, 136 (2016).
- [13] Landucci, F., Jeangros, Q., Rucavado, E., Spori, C., Morales-Masis, M., Ballif, C., Hébert, C. and Hessler-Wyser, A. In *European Microscopy Congress 2016: Proceedings*; Wiley-VCH Verlag GmbH & Co. KGaA (2016).
- [14] Rucavado E., Jeangros Q., Urban D. F., Holovský J., Remes Z., Duchamp M., Landucci F., Dunin-Borkowski R., Körner W., Elsässer C., Hessler-Wyser A., Morales-Masis M. and Ballif C. *In-preparation*, 2017.
- [15] Korner, W., Gumbsch, P., Elsässer, C., "Analysis of electronic subgap states in amorphous semiconductor oxides based on the example of Zn-Sn-O systems," *Phys. Rev. B* 86, 5 (2012).